BULLETIN OF THE EARTHQUAKE
RESEARCH INSTITUTE
Vol. 46 (1968), pp. 361-384

16. *Electromagnetic Induction in Uniform and Non-uniform Sheets Underlain by an Undulating Perfect Conductor.*

By Tsuneji RIKITAKE,

Earthquake Research Institute.

(Read Jan. 23, 1968.—Received Jan. 24, 1968.)

Summary

A theory of electromagnetic induction in uniform and non-uniform thin sheets underlain by a perfect conductor having an undulatory surface is advanced. The uniform sheet behaves as if it is non-uniform, i.e. its resistance is apparently high over the rise of the underlying conductor and is low over the depression. The total (inducing plus induced) Z field (normal to the sheet) is smaller over the former portion of the underlying conductor than over the latter.

A non-uniform sheet representing the low-conducting land, high-conducting deep ocean and transitional sea of which the depth gradually increases is assumed. The underlying perfect conductor is assumed either to upheave (Case A) or subside (Case B) beneath the high-conducting portion of the sheet. Circulation of the induced currents around the high-conducting portion for most of the time is brought out by the calculation though the effect of the underlying conductor can also be seen when the current intensity becomes small in the course of one cycle of variation. Marked enhancement of the Z field around the edge of the deep sea occurs for both the cases. The position of the maximum Z for Case A takes place closer to the coast-line than that for Case B. Geomagnetic variations at a land-ocean boundary seem to be seriously affected by the undulation of the mantle conducting layer.

1. Introduction

Geomagnetic and geoelectric observations on land stations near coast-lines and on the sea floor brought out evidence that the depth of the high-conducting layer of the mantle is different from place to place. Larsen and Cox[1] and Filloux[2], who worked off California, concluded

1) J. LARSEN and C. COX, *J. Geophys. Res.*, **71** (1966), 4441.
2) J. H. FILLOUX, *Thesis. Univ. of California* (1967).

that a high-conducting layer lies very close to the sea bottom there. The top surface of the layer seems likely to dip down toward the American continent somewhere beneath the Californian coast.

Schmucker et al[3], who made an extensive variographic observation in Peru, found no pronounced coastal anomaly of the Z (vertical component of the geomagnetic field) variations as has been found by Schmucker[4] in California. At one of the stations very close to the deep sea, they found that ΔZ for geomagnetic bays is opposite in sign from that due to the usual coastal anomaly. In order to account for such a reverse coast effect, it was imagined that the high-conducting mantle under the Pacific Ocean off Peru must be deeper than that under the land.

A deepening of the mantle conducting layer seems also likely to exist beneath the land-side of the Nova Scotia coast-line as found by variographic observations.[5]

In the light of these findings, the writer thinks that it would be important to examine the effect of a conducting mantle layer having an undulatory surface on geomagnetic variations. Although the induction of electric currents in a semi-infinite conductor having an undulatory surface has been studied by the present writer[6], it would be necessary to take the influence of the overlying sea into account because the upheavals and subsidences are likely to be associated with land-ocean boundaries.

In this paper will be advanced a theory of electromagnetic induction which can be applied either to uniform or non-uniform plane sheets underlain by a perfect conductor having a sinusoidally undulating surface. The assumption of perfect conductivity would be a good approximation as long as we are concerned with a geomagnetic variation having a period of a few tens of minutes and a wavelength of a few thousand kilometers. The theory essentially relies on a method representing the induced currents and fields with sums of Fourier harmonics of finite number, so that no accurate solutions representing very local behaviours of the induced field would be obtained.

Following the description of the theory in Section 2, the resistance in the sheet and the shape of the underlying conductor, which will be taken as one of the likely models, will be referred to in Section 3. In

3) U. SCHMUCKER et al, *Carnegie Inst. Wash. Year Book*, **63** (1964), 354.
4) U. SCHMUCKER *J. Geomag. Geoeletr.*, **15** (1964), 193.
5) S. P. SRIVASTAVA, *Personal communication*, 1967.
6) T. RIKITAKE, *Bull. Earthq. Res. Inst.*, **43** (1965), 161.

Section 4 will be given a test solution of the computer programme. The results for the uniform sheet model and for the non-uniform sheet models will be described in Sections 5 and 6. Some discussion about the theoretically important points will be made in relation to the observed data in Section 7.

2. Theory

Let us think of a system of conductors as shown in Figs. 1a and 1b. In the non-conducting regions, both above and beneath the non-

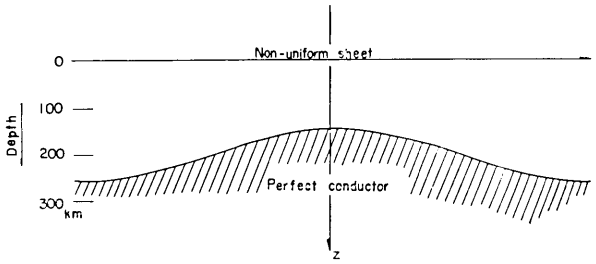

Fig. 1a. Model A of conductors.

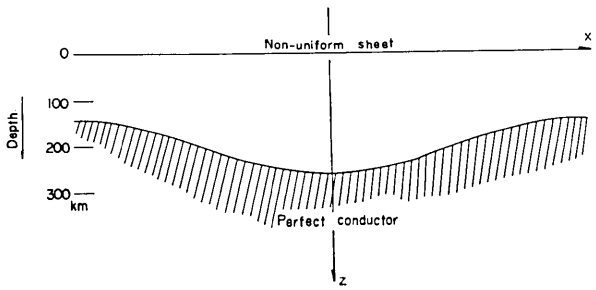

Fig. 1b. Model B of conductors.

uniform sheet, we can define magnetic potential W which satisfies $\nabla^2 W=0$. On assuming a typical inducing field, which is uniform in the x-direction, as given by

$$W_e = Ae^{-qz}\cos qy \ , \tag{1}$$

the magnetic potential for $z<0$ can be written as

$$W_1 = \left[Ae^{-qz} + \sum_m e^{\sqrt{m^2p^2+q^2}z}\, i_m \cos mpx\right]\cos qy \ , \tag{2}$$

on the assumption that the resistance in the sheet at $z=0$ varies

symmetrically about the origin only in the x-direction.

Meanwhile, the magnetic potential in the region between the sheet and the underlying conductor can be written as

$$W_2=\sum_m (e^{-\sqrt{m^2p^2+q^2}z}\, e'_m + e^{\sqrt{m^2p^2+q^2}z}\, i'_m)\cos mpx \cos qy\ . \tag{3}$$

The current function of the electric currents induced in the sheet can be expressed as

$$\Psi=\sum_m K_m \cos mpx \cos qy\ . \tag{4}$$

The continuity condition of the magnetic field at the sheet leads to

$$\left.\begin{aligned} \lambda A + i_m &= e'_m + i'_m + 4\pi K_m\ , \\ \lambda A - i_m &= e'_m - i'_m\ , \end{aligned}\right\} \tag{5}$$

where

$$\lambda=1 \text{ for } m=0\ , \qquad \lambda=0 \text{ for } m\neq 0\ . \tag{6}$$

Denoting the surface of the perfect conductor, which is also uniform in shape in the y-direction and symmetric about the origin in the x-direction, by

$$z=f(x) \tag{7}$$

where $f(x)$ is an even function of x, the condition that the magnetic field normal to the surface vanishes is written as

$$-\frac{df}{dx}H_y + H_z = 0 \qquad \text{at } z=f(x)\ , \tag{8}$$

where H_x and H_z are the field components.

As we obtain from (3) the field components as

$$\left.\begin{aligned} H_x &= \sum_m mp(e^{-\sqrt{m^2p^2+q^2}z}\, e'_m + e^{\sqrt{m^2p^2+q^2}z}\, i'_m)\sin mpx \cos qy\ , \\ H_z &= \sum_m \sqrt{m^2p^2+q^2}\,(e^{-\sqrt{m^2p^2+q^2}z}\, e'_m - e^{\sqrt{m^2p^2+q^2}z}\, i'_m)\cos mpx \cos qy\ , \end{aligned}\right\} \tag{9}$$

(8) is rewritten as

$$\begin{aligned} \sum_m [e^{-\sqrt{m^2p^2+q^2}f}\{\sqrt{m^2p^2+q^2}\cos mpx - (df/dx)mp \sin mpx\}e'_m \\ - e^{\sqrt{m^2p^2+q^2}f}\{\sqrt{m^2p^2+q^2}\cos mpx + (df/dx)mp \sin mpx\}i'_m] = 0\ . \end{aligned} \tag{10}$$

If (10) is multiplied by $\cos Mpx$ and integrated from $-\pi/p$ to π/p with respect to x, we obtain

$$\sum_m [(U_1^M - V_1^M)e'_m - (U_2^M + V_2^M)i'_m] = 0 \ , \tag{11}$$

in which

$$\left.\begin{aligned} U_1^M &= \sqrt{m^2+q^2/p^2}\int_{-\pi}^{\pi} e^{-\sqrt{m^2+q^2/p^2}\,g(s)} \cos ms \cos Ms\, ds \ , \\ U_2^M &= \sqrt{m^2+q^2/p^2}\int_{-\pi}^{\pi} e^{\sqrt{m^2+q^2/p^2}\,g(s)} \cos ms \cos Ms\, ds \ , \\ V_1^M &= m\int_{-\pi}^{\pi} e^{-\sqrt{m^2+q^2/p^2}\,g(s)}(dg/ds) \sin ms \cos Ms\, ds \ , \\ V_2^M &= m\int_{-\pi}^{\pi} e^{\sqrt{m^2+q^2/p^2}\,g(s)}(dg/ds) \sin ms \cos ms\, ds \ , \end{aligned}\right\} \tag{12}$$

and

$$g(s) = pf(s) \ . \tag{13}$$

The condition that should be satisfied at the sheet ($z=0$) is given as follows;

$$\rho(\partial^2\Psi/\partial x^2 + \partial^2\Psi/\partial y^2) + (d\rho/dx)(\partial\Psi/\partial x) = \partial^2 W_1/\partial z\partial t \qquad \text{at } z=0 \ , \tag{14}$$

where ρ is the reciprocal of the electrical conductivity integrated over the thickness of the sheet. (14) reduces to

$$\begin{aligned} &\sum_m [\rho(m^2p^2+q^2)\cos mpx + mp(d\rho/dx)\sin mpx]K_m \\ &\quad = \partial[Aq - \sum_m \sqrt{m^2p^2+q^2}\, i_m \cos mpx]/\partial t \ . \end{aligned} \tag{15}$$

Multiplication and integration operation by $\cos Mpx$ similar to those before leads to

$$\sum_m (A_1^M + A_3^M)K_m = (2\pi/\rho_0 p)d(\lambda(q/p)A - \sqrt{M^2+q^2/p^2}\, i_M)/dt \ , \tag{16}$$

where, defining a typical resistance ρ_0, we put

$$\rho_1 = \rho/\rho_0 \tag{17}$$

and

$$\left.\begin{aligned} A_1^M &= (m^2+q^2/p^2)\int_{-\pi}^{\pi} \rho_1(s)\cos ms \cos Ms\, ds \ , \\ A_3^M &= m\int_{-\pi}^{\pi} (d\rho_1/ds)\sin ms \cos Ms\, ds \ . \end{aligned}\right\} \tag{18}$$

Solving e'_m and i'_m from (5), we obtain

$$\left.\begin{aligned} e'_m &= \lambda A - 2\pi K_m \ , \\ i'_m &= i_m - 2\pi K_m \ . \end{aligned}\right\} \tag{19}$$

Putting (19) into (11), we have

$$\sum_m [(U_1^M - V_1^M)(\lambda A - 2\pi K_m) - (U_2^M + V_2^M)(i_m - 2\pi K_m)] = 0 \ ,$$

which can be rewritten as

$$\sum_m [2\pi(-U_1^M + V_1^M + U_2^M + V_2^M)K_m - (U_2^M + V_2^M)i_m] = (-U_1^M + V_1^M)A \ . \tag{20}$$

(20) along with (16) provides a set of simultaneous equations solving which we may obtain K_m's and i_m's. Neglecting terms for which $m > 11$, for instance, we have 24 equations for $M = 0, 1, 2, \cdots, 11$, so that 24 unknowns, i.e. $K_0, K_1, \cdots, K_{11}, i_0, i_1, \cdots, i_{11}$, can be solved.

When the underlying conductor is very far from the sheet, i.e. $f \to \infty$ (or $g \to \infty$), U_1^M and V_1^M tend to vanish. In that case, (20) reduces to

$$i_m = 2\pi K_m \ ,$$

so that the problem becomes exactly the same as the induction in the sheet placed in free space.

When the change is purely periodic, we put

$$d/dt = i\alpha, \ (\alpha = 2\pi/T) \tag{21}$$

in (16), where T denotes the period. We also put

$$\left.\begin{aligned} K_m &= \overline{K_m} + iK_m^* \ , \\ i_m &= \overline{i_m} + ii_m^* \ . \end{aligned}\right\} \tag{22}$$

With the aid of (21) and (22), we can have equations separately for the real and imaginary parts of (16) and (20) as follows;

$$\left.\begin{aligned} &\sum_m (A_1^M + A_1^M)\overline{K_m} = 2\beta\sqrt{M^2 + q^2/p^2}\, i_M^* \ , \\ &\sum_m (A_1^M + A_3^M)K_m^* = 2\beta(\lambda Ap/q - \sqrt{M^2 + q^2/p^2}\, \overline{i_M}) \ , \\ &\sum_m [2\pi W^M \overline{K_m} - (U_2^M + V_2^M)\overline{i_m}] = (-U_1^M + V_1^M)A \ , \\ &\sum_m [2\pi W^M K_m^* - (U_2^M + V_2^M)i_m^*] = 0 \ , \end{aligned}\right\} \tag{23}$$

where

$$W^M = -U_1^M + V_1^M + U_2^M + V_2^M \tag{24}$$

and

$$\beta = \pi\alpha/\rho_0 p \ . \tag{25}$$

3. Resistance in the sheet and the shape of the underlying conductor

The resistance distribution in the surface sheet is taken as the same as that in the writer's previous paper[7]. The resistance contrast between the land and the deep sea is taken as 100: 1, where the gradual increase in the sea-depth from the coast-line is also taken into account. In Fig. 2 is shown ρ_1, the dimensionless resistance. In the actual

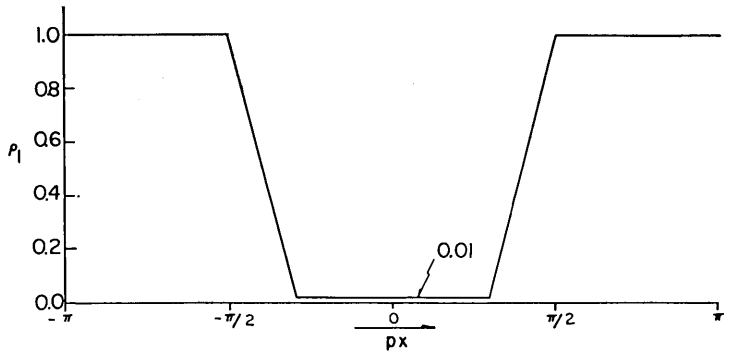

Fig. 2. Distribution of the dimensionless resistance.

numerical work, $p=q$ is assumed. Assuming further that the electrical conductivity of the land amounts to 10^{-13} e.m.u., the total conductivity integrated over a 10 km thickness becomes 10^{-7} e.m.u. ρ_0 is thus taken as 10^7 e.m.u.

Thinking of an inducing field having a wavelength of 40 degrees in longitude at 38° in latitude, $1/p$ is estimated as 0.5577×10^8 cm.

The undulation of the underground perfect conductor is assumed to be sinusoidal with a wavelength equal to that of the inducing field. The mean depth is arbitrarily taken as 200 km and the amplitude is assumed to be equal to 50 km. Two cases in which the conductor upheaves and subsides beneath the sea will be studied.

7) T. RIKITAKE, *Bull. Earthq. Res. Inst.*, **45** (1967), 1229.

Computations of the integrals involved in (12) and (18) are made in a way similar to that in the previous paper[7] for $m=0-11$ and $M=0-11$.

4. Test solutions

The computer programme is tested by applying it to a case in which the surface of the underlying conductor is parallel to the surface sheet of which the conductivity is also uniform.

In that case it is obvious that only an induced field having the same wavelength as that of the inducing field appears. The complex current function coefficient and the internal potential coefficient are readily calculated as

$$\left.\begin{aligned} K_0&=\frac{i\alpha(1-e^{-2qD})}{\rho_0 q+2\pi i\alpha(1-e^{-2qD})}A\ ,\\ i_0&=\left[e^{-2qD}+\frac{2\pi i\alpha(1-e^{-2qD})^2}{\rho_0 q+2\pi i\alpha(1-e^{-2qD})}\right]A\ ,\end{aligned}\right\} \tag{26}$$

where D is the depth of the perfect conductor and ρ_0 the resistance of the surface sheet.

Taking D as 200 km, the period as 1 min. and the other parameters as those as defined in the last section, K_0 and i_0 are from (26) calculated for a unit A as

$$\left.\begin{aligned} 2\pi K_0&=0.7792+0.4148i\ ,\\ i_0&=0.8870+0.2123i\ ,\end{aligned}\right\} \tag{27}$$

which agree with the results of the computer work with an accuracy of $\pm 10^{-4}$ or less. The coefficients for higher harmonic terms are vanishingly small. They are of the order of 10^{-7} or smaller.

5. Uniform sheet over an undulating perfect conductor

In order to see the effect of the undulating underground conductor, it is of interest to examine how the electric currents induced in a uniform surface sheet ($\rho_1=1$) are affected by the undulation. The current function coefficients for periods 1 min. and 10 min. are computed when the perfect conductor is upheaved and subsided symmetrically about the z-axis. The mean depth is assumed as 200 km. Likewise, other parameters are assumed to be the same as those in Section 4. The coefficients for the

upheaved case are given in Table 1.

It is evident from symmetry consideration that the coefficients for the subsided case take on the same and opposite signs respectively for even and odd m's.

In Figs. 3a and 3b are shown the current lines for the two cases at epochs $\alpha t=0, \pi/3$ and $2\pi/3$. It is observed in these figures that the current intensity tends to be most of the time weak above the upheaved portion of the underlying conductor and to encircle the portion of the sheet under which the conductor is subsided. The sheet behaves as if it is non-uniform, i.e. its resistivity being high above the rise of the deep-seated conductor and low above the sink. The intensity of the induced currents is generally larger for the 60 sec. period than that for the 600 sec. period.

The magnetic field over the sheet is readily calculated from (2) with the coefficients i_m's as given in Table 2. The induced magnetic field is produced by the induced currents in the sheet and those flowing on the surface of the underlying conductor. Fig. 4 expresses the changes in the total (inducing plus induced) Z field along the x-axis immediately above the sheet for three epochs, i.e. $\alpha t=0, \pi/3$ and $2\pi/3$. It is seen in the figure that the sheet behaves as a very good conductor for a rapid change having a short period such as 60 sec., so that the induced

Table 1. Current function coefficients (K_m's) in units of $2\pi A$ for the uniform sheet when the underlying perfect conductor is most upheaved beneath the coordinate origin.

m	$T=1$ min.		$T=10$ min.	
	$\overline{K_m}$	K_m^*	$\overline{K_m}$	K_m^*
0	0.77020	0.40261	0.03444	0.18008
1	0.10180	0.06915	0.00539	0.03139
2	0.01490	−0.02432	0.00082	−0.00157
3	−0.00746	−0.00534	−0.00016	0.00007
4	−0.00090	0.00269	0.00002	0.00005
5	0.00091	0.00125	0.00001	−0.00005
6	0.00004	−0.00059	0.00000	0.00001
7	−0.00011	−0.00043	0.00000	0.00001
8	−0.00001	0.00014	0.00000	0.00000
9	0.00001	0.00016	0.00000	0.00000
10	0.00000	−0.00002	0.00000	0.00000
11	0.00000	−0.00006	0.00000	0.00000

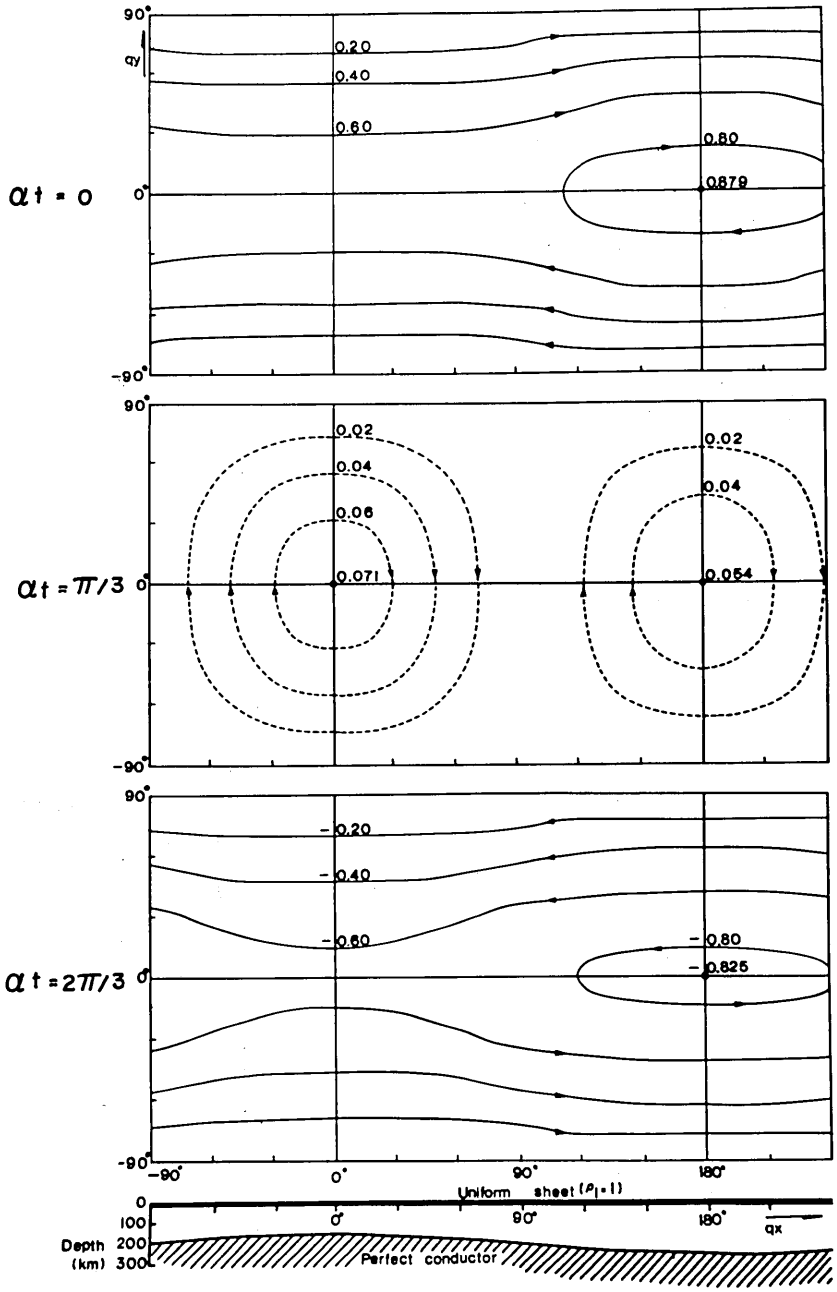

Fig. 3a. Current lines for three epochs induced in the uniform sheet by an inducing field having a period of 1 min.

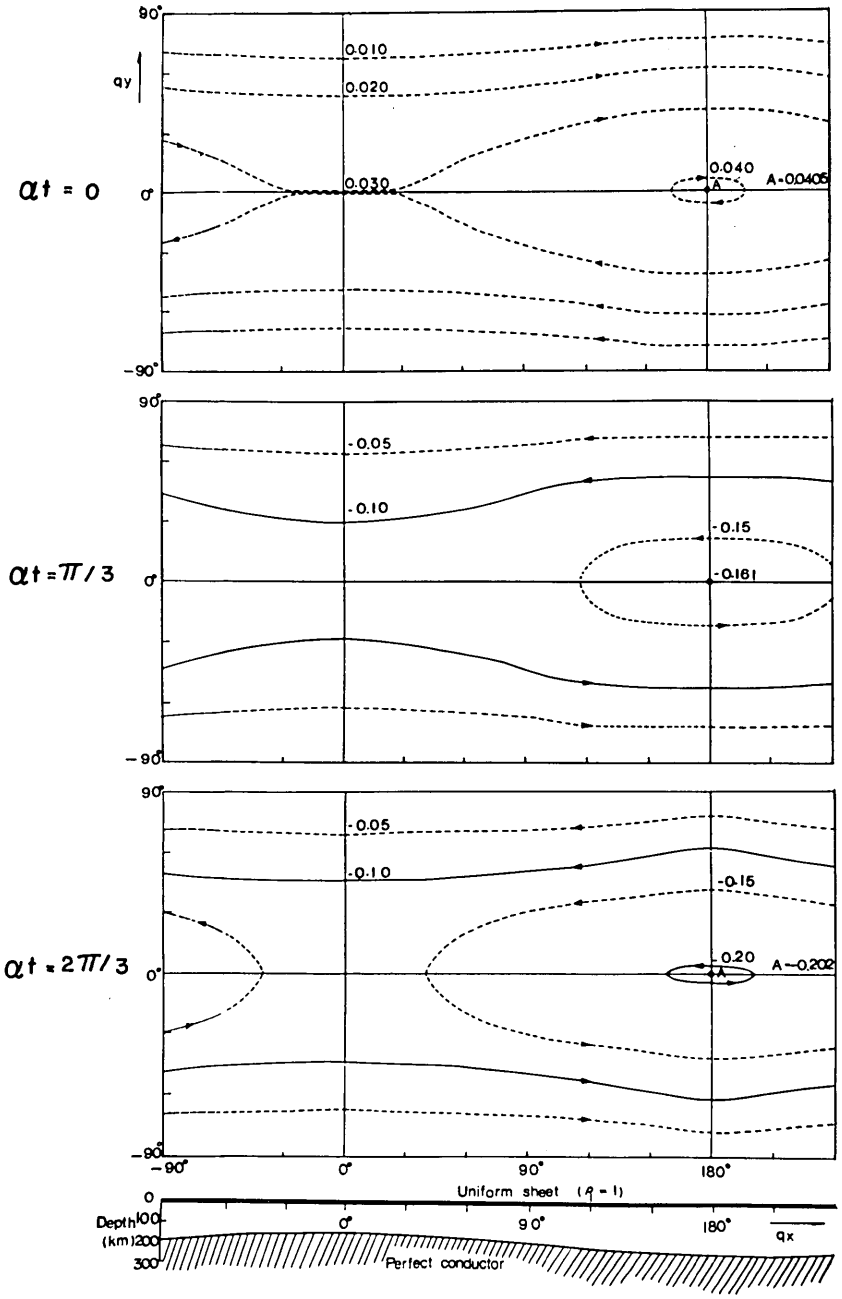

Fig. 3b. Current lines for three epochs induced in the uniform sheet by an inducing field having a period of 10 min.

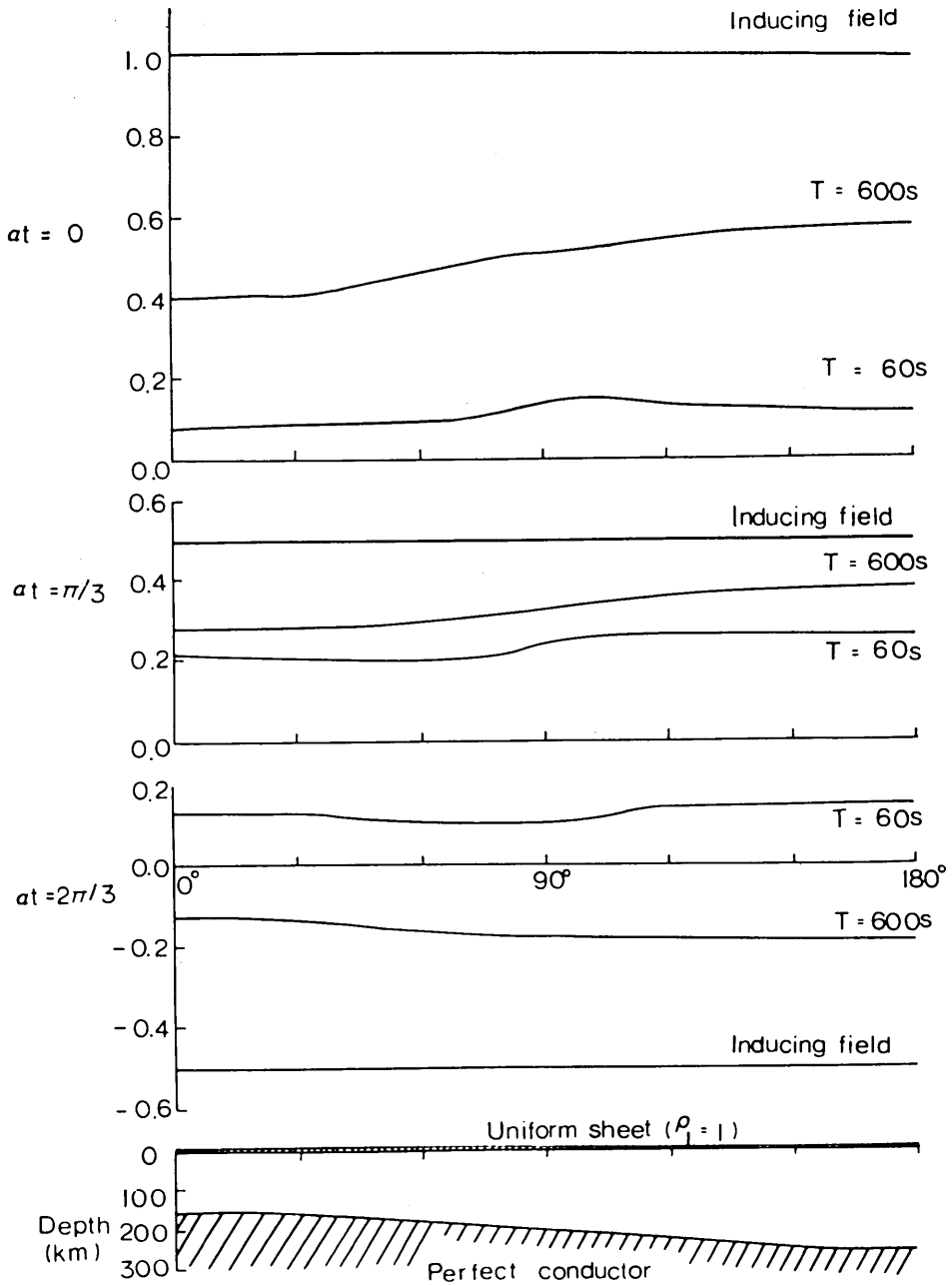

Fig. 4. The Z field distribution for three epochs.

Table 2. Coefficients for the magnetic potential (i_m's) in units of A when the underlying perfect conductor is most upheaved beneath the coordinate origin.

m	$T=1$ min.		$T=10$ min.	
	$\bar{i_m}$	i_m^*	$\bar{i_m}$	i_m^*
0	0.89028	0.20989	0.50924	0.09386
1	−0.01333	0.01962	−0.06048	0.01039
2	0.00741	0.00454	0.00479	0.00249
3	−0.00230	−0.00322	−0.00032	−0.00069
4	−0.00151	−0.00051	−0.00030	0.00009
5	−0.00087	0.00063	0.00034	0.00008
6	0.00049	0.00004	−0.00007	−0.00003
7	−0.00041	−0.00011	−0.00010	0.00003
8	−0.00015	−0.00001	0.00003	−0.00001
9	−0.00019	0.00001	0.00004	−0.00001
10	0.00002	0.00000	0.00005	0.00000
11	0.00009	0.00001	−0.00002	−0.00001

Z cancels most parts of the inducing Z resulting in a small Z over the sheet. Since the screening of the sheet becomes considerable in this case, the influence of the underlying conductor to the surface magnetic field is not outstanding although we see that the amplitude of Z over the subsided portion of the underlying conductor is slightly larger than that over the upheaved portion.

The effect of the underlying conductor appears to become appreciable as the period (T) of geomagnetic variation increases. For the $T=600$ sec. curves, the increase in the amplitude of Z, as we move over to the portion under which the conductor gets deeper, becomes remarkable.

6. Non-uniform sheet over an undulating perfect conductor

Electromagnetic inductions in a non-uniform sheet as described in Section 3 are studied in this section when the underlying conductor upheaves (Case A) and subsides (Case B) beneath the high-conducting portion of the sheet. The coefficients in these cases are calculated as given in Table 3 for $T=60$ sec. and $T=600$ sec.

The convergence of the coefficients in Table 3 is poor compared to that (Table 1) for a uniform sheet. Especially, we see that the coefficients of the higher harmonic terms for Case B do not become appreciably

Table 3. Current function coefficients in units of $2\pi A$ for Cases A and B.

m	Case A				Case B			
	$T=1$ min.		$T=10$ min.		$T=1$ min.		$T=10$ min.	
	$\overline{K_m}$	K_m^*	$\overline{K_m}$	K_m^*	$\overline{K_m}$	K_m^*	$\overline{K_m}$	K_m^*
0	0.95034	0.30630	0.03683	0.40232	0.86593	0.21853	0.30001	0.26426
1	−0.14992	−0.15819	0.13974	−0.21036	−0.37014	0.03684	−0.39641	−0.11753
2	−0.01544	0.06356	−0.11676	0.09632	0.07713	−0.15243	0.24982	−0.02130
3	0.03303	0.00970	0.05837	−0.03264	0.03857	0.03900	−0.11173	0.04380
4	−0.00585	−0.00954	−0.00701	0.00242	−0.03050	0.01743	0.01880	−0.03377
5	−0.00687	−0.00293	−0.01398	0.01114	0.00031	−0.01700	0.02955	0.00619
6	0.00282	0.00080	0.00946	−0.01461	0.01040	0.00435	−0.03015	0.01075
7	0.00137	0.00259	−0.00020	0.00831	−0.00465	0.00404	0.01096	−0.01380
8	−0.00051	−0.00030	−0.00308	0.00184	−0.00201	−0.00453	0.00681	0.00587
9	−0.00046	−0.00129	0.00247	−0.00745	0.00318	0.00086	−0.01393	0.00341
10	0.00010	0.00025	−0.00103	0.00680	−0.00097	0.00170	0.01128	−0.00720
11	0.00007	0.00038	−0.00023	−0.00345	−0.00073	−0.00174	−0.00492	0.00549

small. It is consequently obvious that we need many more harmonic terms in order to properly approximate the current functions and that the coefficients as calculated here involve fairly large errors. In contrast to the induction in a uniform sheet as dealt with in the last section, the resistance contrast in the present non-uniform sheet is enormously large, so that it is quite natural that many harmonic functions are required for expressing the induced currents.

In spite of the crudeness of the solutions, the writer believes that approximate patterns of the induced currents can be illustrated by summing up the harmonic terms although their details are not too reliable. Figs. 5a and 5b are the current systems for Case A with $T=60$ and $T=600$ sec., while Figs. 6a and 6b are those for Case B. Looking at these figures, we notice that the induced currents encircle most of the time the high-conducting portion of the sheet. The current patterns seem much the same as those for the sheet placed in free space as studied in the previous paper[7]. But we also see the effect of the underlying conductor when the current intensity becomes small in the course of one cycle of variation.

The magnitude of the coefficients of higher harmonic terms relative to those of lower ones is larger for Case B than for Case A. This seems to mean that, very roughly speaking, the upheaval of the under-

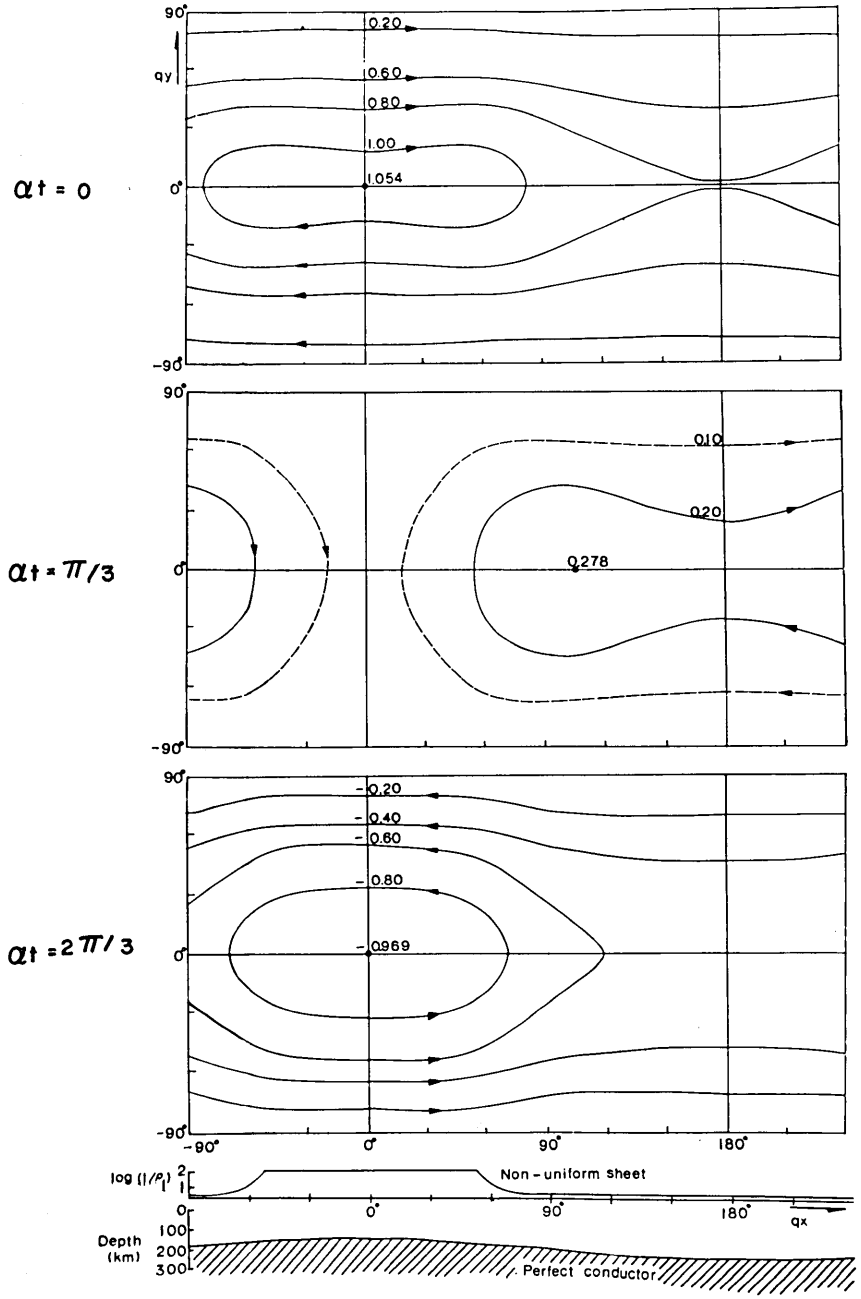

Fig. 5a. Current lines for three epochs for Case A induced in the non-uniform sheet by an inducing field having a period of 1 min.

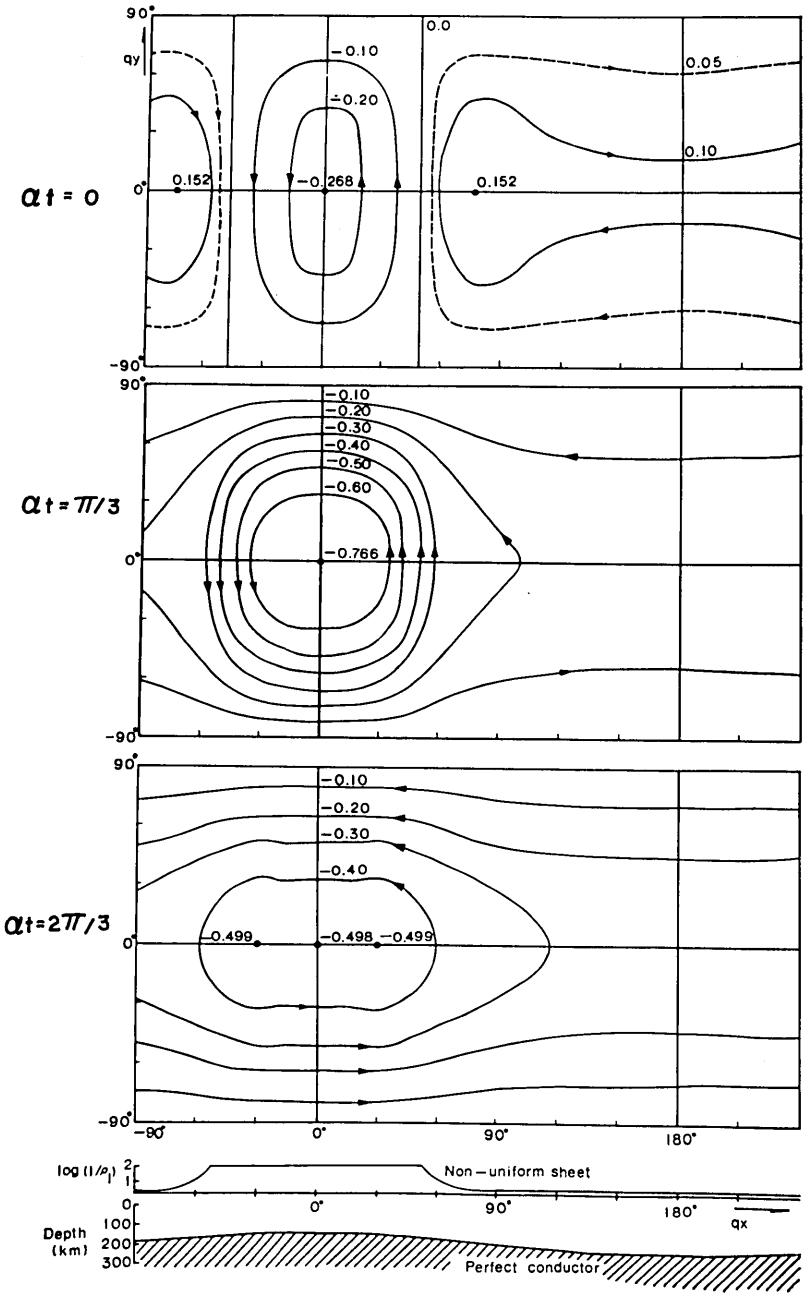

Fig. 5b. Current lines for three epochs for Case A induced in the non-uniform sheet by an inducing field having a period of 10 min.

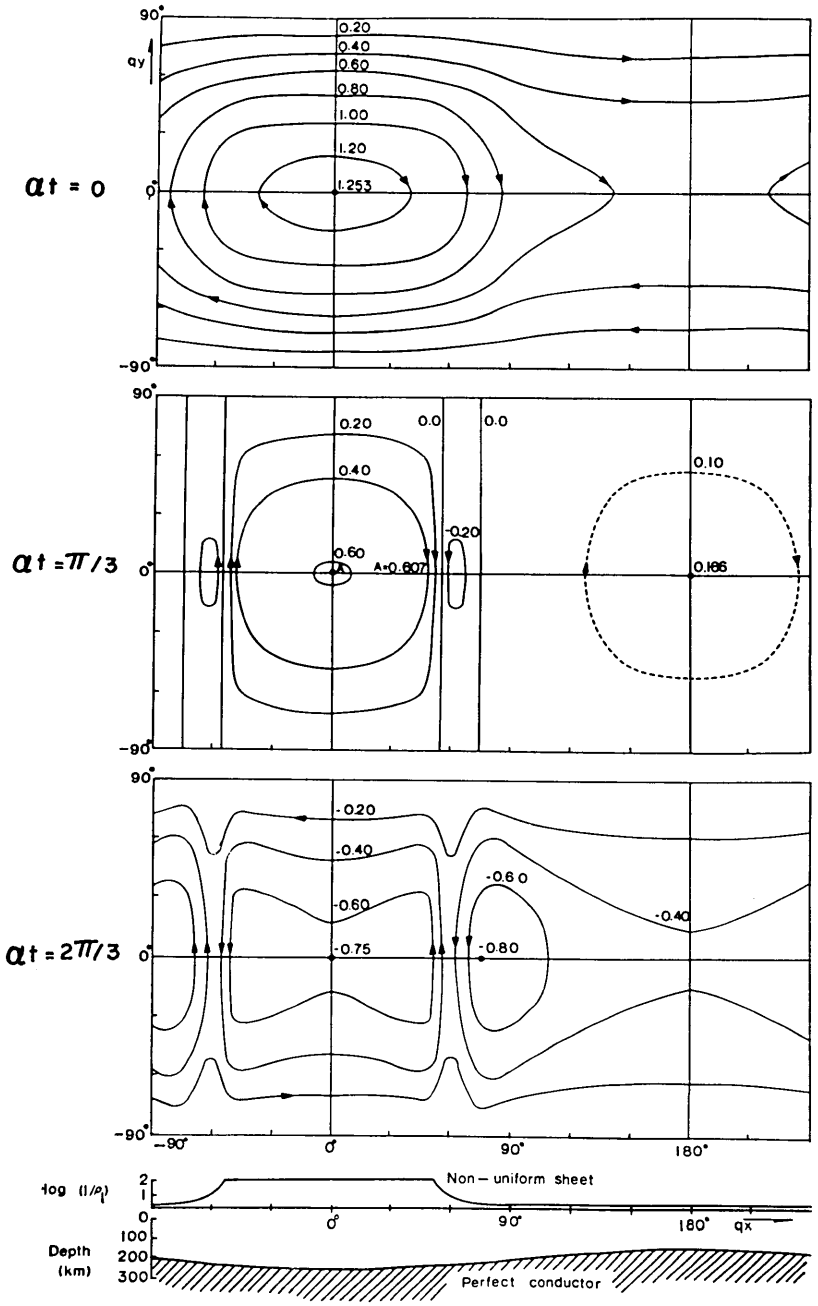

Fig. 6a. Current lines for three epochs for Case B induced in the non-uniform sheet by an inducing field having a period of 1 min.

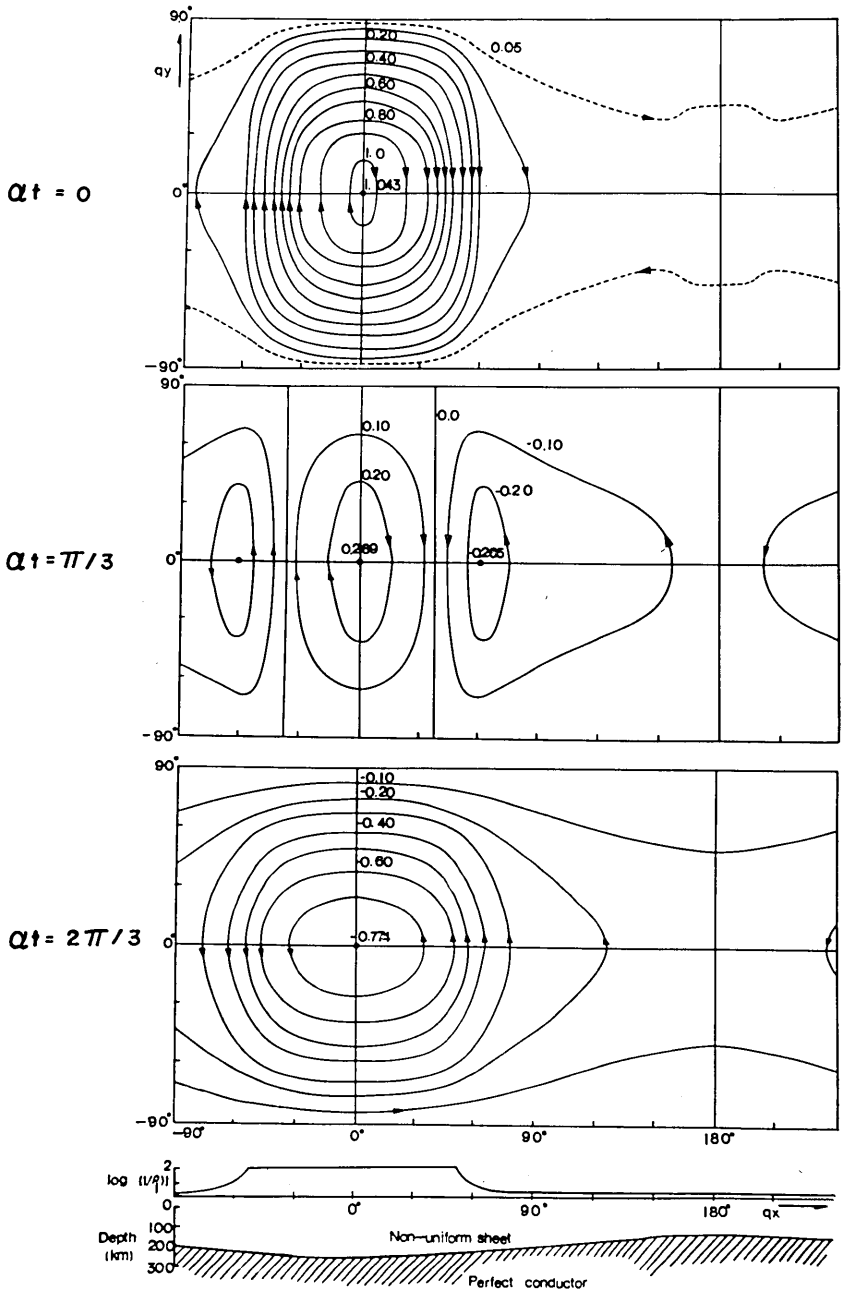

Fig. 6b. Current lines for three epochs for Case B induced in the non-uniform sheet by an inducing field having a period of 10 min.

lying conductor beneath the high-conducting portion of the sheet works in such a way as to lessen the conductivity contrast in the sheet. Meanwhile the subsidence there makes the apparent contrast large.

One of the aims of the calculations in this section is to bring out the distributions of the magnetic field components, especially that of the Z component, over the sheet. Such a study is useful for interpreting a geomagnetic variation anomaly near a coast-line. It is regrettable, however, that the convergence of the coefficients for the induced magnetic potential in both the cases is not quite good.

In Table 4 are given the coefficients for the magnetic potential.

Table 4. Coefficients for the magnetic potential (i_m's) in units of A for Cases A and B.

m	Case A				Case B			
	T=1 min.		T=10 min.		T=1 min.		T=10 min.	
	$\overline{i_m}$	i_m^*	$\overline{i_m}$	i_m^*	$\overline{i_m}$	i_m^*	$\overline{i_m}$	i_m^*
0	0.96416	0.14048	0.52091	0.18893	0.95773	0.10950	0.67073	0.14293
1	−0.00436	0.03355	−0.08686	0.04816	0.00010	0.01233	0.008907	−0.01149
2	−0.00051	−0.01651	0.04871	−0.00409	0.02142	−0.01033	0.06447	0.00995
3	−0.00879	0.00556	−0.03173	0.01597	0.00093	0.01479	−0.03798	0.02280
4	0.00156	0.00560	−0.01009	0.02378	−0.00986	−0.00111	0.01642	−0.00137
5	0.00631	−0.00606	0.02660	−0.02863	0.00145	−0.00885	0.02270	0.01189
6	−0.00170	−0.0113	0.00006	−0.01054	0.00401	0.00507	−0.01644	0.00640
7	−0.00334	0.00379	−0.01588	0.02710	−0.00286	0.00265	0.00696	−0.01334
8	0.00092	−0.00020	0.00069	−0.00211	−0.00055	−0.00404	0.00381	0.00498
9	0.00144	−0.00166	0.00890	−0.01484	0.00215	0.00084	−0.01154	0.00393
10	−0.00008	0.00025	−0.00163	0.00781	−0.00113	0.00157	0.01118	−0.00675
11	−0.00071	0.00050	−0.00275	−0.00086	−0.00033	−0.00163	−0.00542	0.00493

The magnetic fields, which are calculated by differentiating the magnetic potential, are seriously affected by errors of the higher harmonic terms, so that no accurate estimation of the field components would be possible to make unless we take more harmonic terms.

The writer nevertheless thinks that a rough estimate of the field components could be made even by the present method provided we do not put much stress on the details of their distributions. In Fig. 7a and 7b are illustrated the total Z field distribution along the x-axis for the three epochs respectively for Cases A and B. It is observed in these figures that the Z for T=60 sec. is generally smaller in magnitude

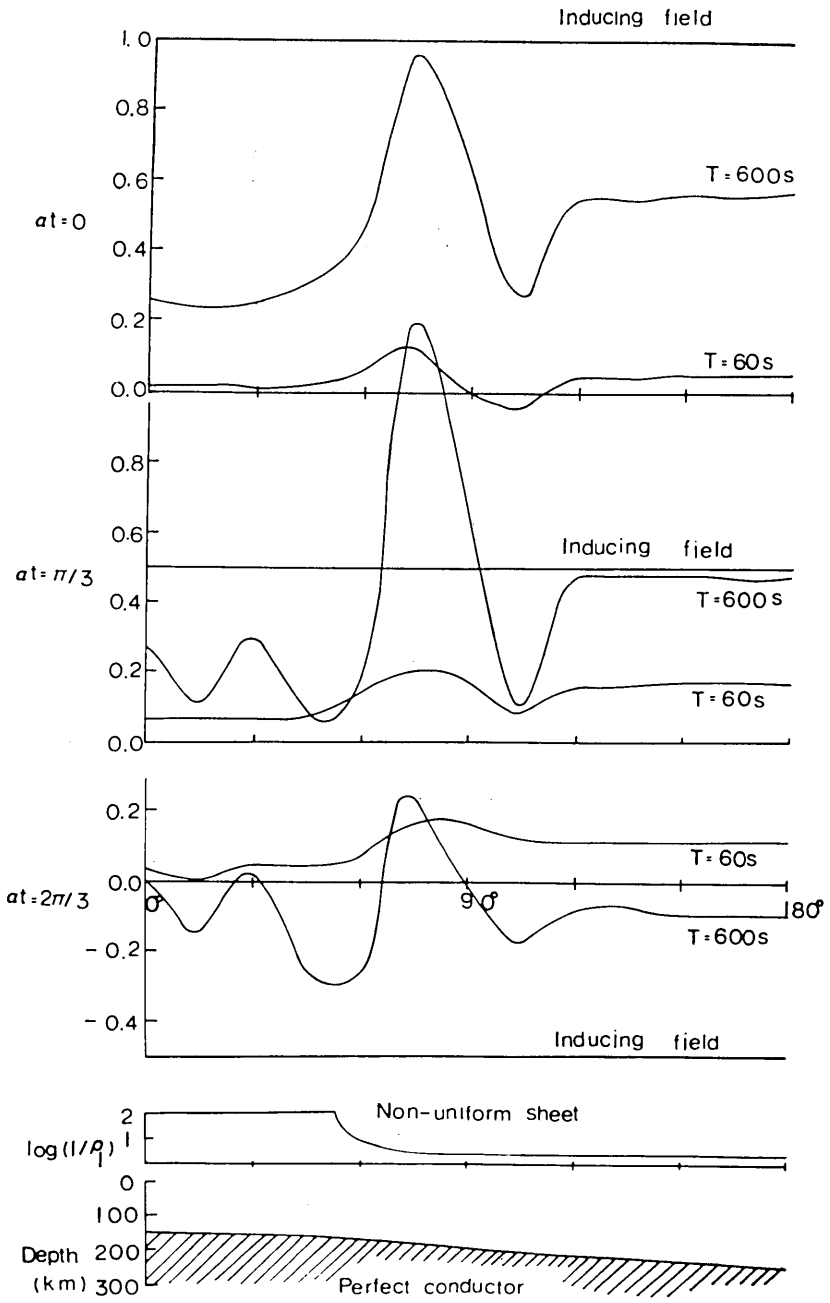

Fig. 7a. The Z field distribution for three epochs for Case A.

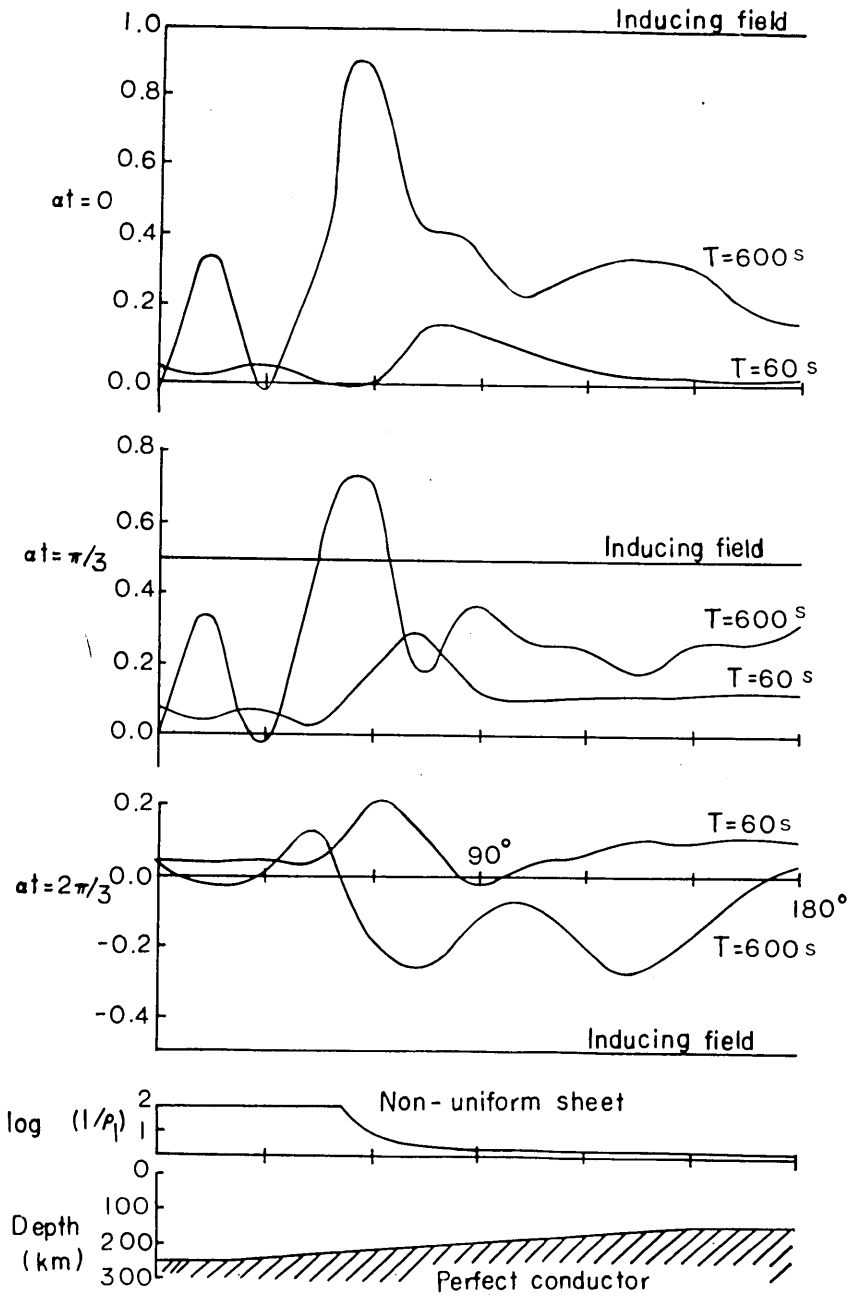

Fig. 7b. The Z field distribution for three epochs for Case B.

than that for $T=600$ sec. The fact can be understood if one thinks of the tendency that a sheet reacts as a nearly perfect conductor for a very short period variation. Close examination of the curves for $T=60$ sec. makes us notice that the Z field over the high-conducting portion of the sheet is smaller than that over the low-conducting one. In any case for $T=60$ sec, we observe an enhancement of the Z amplitude on the slope which connects the low-conducting portion of the sheet to the high-conducting portion.

The fluctuations of the Z distributions for $T=600$ sec. make us suspect that they are caused by errors involved in the coefficients of higher harmonic terms. In should be pointed out, however, that we observe an enormous enhancement of the Z field in between the high- and low-conducting portions of the sheet although the extent of the enhancement would not be quantitatively correct. The enhancement seems to be larger for Case A than for Case B. The maximum of the enhanced Z seems to be somewhat displaced towards the high-conducting portion for Case B. It has been known for the same sheet placed in free space that the maximum anomaly in Z takes place still close to the edge of the high-conducting portion of the sheet. The behaviours of the Z field as seen here may change for other combinations of the configuration of conductors.

7. Discussion and concluding remarks

The present calculation of electromagnetic induction in a uniform sheet over a sinusoidally undulating perfect conductor proves that, as far as the induced currents in the sheet are concerned, the sheet reacts to an inducing field as if it is non-uniform, i.e. its resistance is apparently high above the rise and low above the depression of the underlying conductor. It is not easy to see intuitively how the magnetic field is distributed over the sheet because the field consists of the contributions from the induced currents flowing both in the sheet and at the surface of the perfect conductor. The calculated distribution indicates, however, that the induced field is large over the upheaved portion of the underlying conductor and small over the subsided portion. The total (inducing plus induced) Z field therefore stays low and high respectively above the rise and depression of the underlying conductor although such a statement is not quite exact because of the phase lag of the induced field behind the inducing one. The present study suggests a possibility of detecting

a suboceanic mantle layer of high conductivity by observing changes in the geomagnetic field and earth-currents.

The writer's intention of investigating possible influence of the undulatory mantle layer on goemagnetic variations is not quite successful because the method of approximation by expressing the current functions and induced magnetic fields with twelve harmonic functions is not accurate enough. But the relation between the Z field and the undulation of the underlying conductor in the last paragraph seems to hold good for the parts of the sheet far from its high-conducting portion.

Nothing definite can be said about the influence of the underlying conductor on the Z field distribution over the high-conducting portion of the sheet, which simulates a deep ocean, because of the poor convergence of the series. The only thing which may be concluded from the present study would be the enhancement of the Z field around the edge of the deep ocean. It is interesting to note that the maximum enhancement of Z occurs in between the deep sea and coast-line when the deep conducting layer upheaves seawards (Case A). When the layer dips down seawards (Case B), the position of the Z maximum considerably shifts towards the edge of the deep sea, so that no marked decrease in Z would be observed at inland stations in this case.

It has been suggested that the configuration of conductor system around the Californian coast-line would be something like that of Case A although a mantle layer of high conductivity shallower than the present model would be a better approximation. The strong coastal effect of Z as has been observed there qualitatively harmonizes with the theoretically expected distribution of the magnetic field as studied in this paper.

No reverse coastal effect has been found by the calculation for Case B which may be an example of an underground model suggested for the Pacific coast of Peru. Whether or not we can have a reverse coastal effect as reported by Schmucker et al[3] by modifying the underground structure model in a reasonable range is not known. But it should be pointed out that even the present model does suggest that no marked coastal effect is observed at a station on the coast-line or at those further inland.

The present study indicates that an undulatory subsurface conducting layer largely affects the magnetic field variations around the land-sea boundaries as well as the electric currents in the ocean. The writer believes, therefore, that an intensive investigation into geomagnetic and

geoelectric variations over land-sea boundaries may lead to a better understanding of undergound electrical structure beneath continental margins.

---

16. 起伏のある導体上におかれた薄層の電磁感応

地震研究所　力　武　常　次

正弦波状の凹凸のある完全導体上に一様または非一様薄層がある場合の電磁感応を調べた．

はじめの場合は，一様な深さの海洋底の導電的マントルに起伏がある場合に相当するが，誘導電流は凸起部上の層中で小さくなる．またそこでは磁場の鉛直分力（層に直交する成分）が小さくなる．このような結果から，海上で磁場変動を観測することにより，マントルの凸凹を検出することの可能性が示唆される．

つぎに薄層が深海に対応する高導電的，大陸棚に対応する漸増導電的および大陸に対応する低導電的部分からなる場合について，マントル隆起部が高導電部下にあるとき (Case A) と沈降部がそこにあるとき (Case B) とを調べた．電流分布の様子は，この薄層が free space におかれた場合と似ていて，高導電部分を環流する．二つの場合とも，高導電部分の端で鉛直分力がいちじるしく増大するが，その最大の位置は Case A については，Case B よりも低導電部分にかたよる．このような結果からみて，海陸境界付近の地球磁場変動を詳しく観測することによつて，continental margin の地下の電気的構造を知ることの可能性が示唆される．